PNAS RESEARCH ARTICLE | PHYSIOLOGY

TRPV1 corneal neuralgia mutation: Enhanced pH response, bradykinin sensitization, and capsaicin desensitization

Roberta Gualdani[a], Solène Barbeau[a], Jun-Hui Yuan[b,c,d], Deborah S. Jacobs[e], Philippe Gailly[a], Sulayman D. Dib-Hajj[b,c,d], and Stephen G. Waxman[b,c,d,1]

Edited by David Julius, University of California, San Francisco, CA; received March 26, 2024; accepted July 30, 2024

The factors that contribute to pain after nerve injury remain incompletely understood. Laser-assisted in situ keratomileusis (LASIK) and photorefractive keratectomy (PRK) are common surgical techniques to correct refractive errors. After LASIK or PRK, a subset of patients suffers intense and persistent pain, of unknown origin, described by patients as feeling like shards of glass in their eye. Here, we evaluated a TRPV1 variant, p.V527M, found in a 49-y-old woman who developed corneal pain after LASIK and subsequent PRK enhancement, reporting an Ocular Surface Disease Index score of 100. Using patch-clamp and Ca^{2+} imaging, we found that the V527M mutation enhances the response to acidic pH. Increasing proton concentration induced a stronger leftward shift in the activation curve of V527M compared to WT, resulting in channel activity of the mutant in acidic pH at more physiological membrane potentials. Finally, comparing the responses to consecutive applications of different agonists, we found in V527M channels a reduced capsaicin-induced desensitization and increased sensitization by the arachidonic acid metabolite 12-hydroxyeicosatetraenoic acid (12-HETE). We hypothesize that the increased response in V527M channels to protons and enhanced sensitization by 12-HETE, two inflammatory mediators released in the cornea after tissue damage, may contribute to the pathogenesis of corneal neuralgia after refractive surgery.

TRP channels | human mutation | corneal neuralgia

Significance

This study explores the contribution of the TRPV1 mutation V527M in the development of corneal neuralgia after refractive surgery. Our data show that V527M causes susceptibility to neuropathic pain by increasing the excitability of trigeminal ganglion neurons, enhancing sensitivity to bradykinin and protons, two inflammatory mediators released after trigeminal nerve injury, and decreasing capsaicin-induced desensitization in trigeminal ganglion neurons.

Neuropathic pain (NeP) is defined as pain caused by a disease or injury to the somatosensory nervous system, which underlies the perception of touch, pressure, pain, temperature, position, and vibration (1, 2). A number of different diseases, injuries, or medications (e.g., diabetes, surgery, trauma, nerve compression, use of chemotherapeutic agents) can affect the peripheral and/or central nervous system (3), causing an alteration in nociceptive signaling and modulation leading to increased sensitivity and pain. These types of injury can alter the function of sensory nerves and increase excitatory input into the spinal cord, where alterations in the balance of excitatory and inhibitory modulation can result in enhanced excitability and pain (4). Although NeP represents a disabling condition that affects millions of patients worldwide, the therapies available to treat it are often inadequate. This may be due to lack of diagnostic accuracy, insufficient understanding of the pathophysiological mechanisms of pain, relative ineffectiveness of medications, and/or side effects of existing drugs (3).

A better understanding of interindividual differences in susceptibility to NeP (5–8) is also needed. We recently analyzed two mutations of transient receptor potential (TRP) channels found in patients affected by trigeminal neuralgia (9, 10), showing that both mutations contribute to abnormal hyperexcitability of trigeminal ganglion neurons, which may predispose the carriers to the development of pain (11, 12). However, the observation that both mutations were also found in unaffected siblings (13) suggests that these mutations are not causal per se but instead act as risk factors in a multihit model.

Persistent postsurgical pain provides a model in which the exogenous insult is well defined and can be temporally linked to the onset of pain (14, 15). Persistent pain after laser-assisted in situ keratomileusis (LASIK) and photorefractive keratectomy (PRK), two surgical techniques commonly used to correct myopia, provides a model in which there is reproducible injury into trigeminal afferents. In LASIK, the distal axons of trigeminal ganglion sensory neurons within the cornea are transected; in PRK, nerves in the subbasal plexus and some stromal processes are ablated. After these procedures, a small subset of patients develops intense and persistent pain, described by patients as feeling like shards of glass in their eye (16). NeP following refractive surgery is rare; there are no population data on prevalence. A recent retrospective series reviewing approximately 16,000 LASIK cases performed by a single surgeon from 1996 to 2021 identified 18 instances of

Author affiliations: [a]Laboratory of Cell Physiology, Institute of Neuroscience, Université catholique de Louvain, Brussels B-1200, Belgium; [b]Department of Neurology, Yale School of Medicine, New Haven, CT 06520; [c]Center for Neuroscience and Regeneration Research, Yale School of Medicine, New Haven, CT 06520; [d]Neurorehabilitation Research Center, Veterans Affairs Medical Center, West Haven, CT 06516; and [e]Department of Ophthalmology, Massachusetts Eye and Ear, Boston, MA 02114

Author contributions: R.G., P.G., S.D.D.-H., and S.G.W. designed research; R.G. and S.B. performed research; R.G., P.G., S.D.D.-H., and S.G.W. contributed new reagents/analytic tools; R.G., S.B., P.G., S.D.D.-H., and S.G.W. analyzed data; and R.G., J.-H.Y., D.S.J., P.G., S.D.D.-H., and S.G.W. wrote the paper.

The authors declare no competing interest.

This article is a PNAS Direct Submission.

[1]To whom correspondence may be addressed. Email: stephen.waxman@yale.edu.

Published September 3, 2024.

neuropathic corneal pain that occurred postprocedure, which is 1/900 cases, or occurrence of 0.11%, with no reports on PRK enhancement among those cases (16).

A recent study investigated the contribution of genomic factors to corneal neuralgia after refractive surgery (17), revealing, through whole exome sequencing (WES) analysis, multiple variants in electrogenisome-related ion channel and collagen gene panels. Many of these variants belong to TRP channels, widely expressed in sensory nerve terminals innervating the eye.

In the present study, we analyzed a mutation of the Transient receptor potential vanilloid 1 (TRPV1) channel, p.V527M, found in a woman who had LASIK in both eyes at age 30. She subsequently had a PRK procedure, in both eyes, at age 49. Four weeks later, she developed severe, persistent pain in both eyes, reporting the maximum Ocular Surface Disease Index (OSDI) score of 100.

TRPV1 is a nonselective Na^+- and Ca^{2+}-permeable cation channel found primarily in trigeminal and dorsal root ganglion nociceptors (18). This polymodal receptor detects a wide range of thermal and chemical painful stimuli, playing a significant role in nociception (19). It is activated by noxious heat (>42 °C), protons (low pH), voltage, plant and animal toxins, and bioactive lipids (20). Activators of TRPV1 engage several binding domains, among them the intracellular vanilloid binding site located between S3 and S4, to which capsaicin, a vanilloid found in chili peppers, and endogenous bioactive lipids, produced mainly during inflammation, bind (20–22). Early mutagenesis studies (21, 23) and the more recent cryo-EM structures of the channel (24, 25) have shown that the residues Y511, S512, and T550 are critical for channel activation by capsaicin. Capsaicin binds to the vanilloid pocket assuming a "tail up, head down" configuration and the binding is mediated both by hydrogen bonds that stabilize capsaicin head, and by van der Waals interactions between the capsaicin tail and residues along the transmembrane region (24, 25).

TRPV1 is mainly expressed in a specific subgroup of polymodal nociceptors, small-diameter unmyelinated C fibers, which are slow-conducting, and express calcitonin gene-related neuropeptides and substance P (26). TRPV1 activation in nociceptive neurons leads to an increase in cytosolic Ca^{2+}, subsequent depolarization, and release of inflammatory peptides from primary afferent nerve terminals (27). TRPV1 is also activated by a variety of inflammatory mediators such as cytokines, prostaglandins, bradykinins (BK), and neurotrophins that act on their specific receptors by indirectly modulating TRPV1 through intracellular signaling pathways (28).

In this study, we explored the biophysical properties of the TRPV1 mutation V527M found in a patient affected by corneal NeP and studied the effect of this mutation on excitability of trigeminal ganglion neurons. We found that V527M exhibits an enhanced response to acidic pH and heat and a reduced capsaicin-induced desensitization. Trigeminal neurons expressing V527M showed an enhanced response to acidic pH and increased sensitization by BK due to a higher affinity of the mutant channel for the arachidonic acid (AA) metabolite, 12-hydroxyeicosatetraenoic acid (12-HETE), one of the inflammatory mediators released in the cornea after tissue damage.

Results

V527M Enhances Response to Acidic pH and Heat. The heterozygous missense variant c.1579G>A results in the substitution of valine by methionine at p.527 in transmembrane segment 3 of the TRPV1 channel (p. Val527Met). The residue is located near the vanilloid binding pocket, where exogenous vanilloid ligands, such as capsaicin, and endogenous bioactive lipids bind (Fig. 1*A*). Human embryonic kidney (HEK) 293 cells were transiently transfected with plasmids encoding hTRPV1 wild-type (WT) and V527M and green fluorescent protein (GFP)-positive cells were analyzed by Ca^{2+} imaging and patch-clamp experiments.

First, by performing Fura-2 experiments, we tested the response of TRPV1 to capsaicin and acidic pH to understand whether the mutation affects TRPV1 agonist response leading to a gain-of-function or loss-of-function phenotype.

External application of 250 nM capsaicin evoked a large and similar in amplitude increase of $[Ca^{2+}]_i$ in both WT and V527M channels (Fig. 1 *B* and *D*). On the contrary, Ca^{2+} influx in response to acidic pH (5.5) elicited a significantly larger response in V527M mutant compared to WT channels (Fig. 1 *C* and *E*). These results were confirmed by patch-clamp experiments. Whole-cell currents were elicited by a voltage ramp protocol ranging from −100 to +100 mV and TRPV1 currents were activated by perfusion with a solution containing capsaicin and acidic solution, respectively (Fig. 1 *F* and *J*). Capsaicin activation elicited a current of similar amplitude in WT and V527M channels (Fig. 1 *G* and *H*), and the capsaicin dose–response curves revealed similar EC_{50} values for WT and mutant receptors (267 ± 55 nM and 248 ± 34 nM, respectively, Fig. 1*I*). On the contrary, the response to acidic pH was significantly higher in V527M mutant than in WT channels (Fig. 1 *K* and *L*). Finally, we investigated the effects of V527M mutation on TRPV1 heat activation properties, by recording whole-cell currents in response to a heat ramp from room temperature to 45 °C. Activation by heat was markedly elevated in the mutant compared with WT (Fig. 1 *M* and *N*). Overall, these results suggest that V527M is a gain-of-function mutation for acidic pH and heat, but not for capsaicin.

V527M Affects pH-Mediated Channel Gating. Since protons act as inflammatory mediators released during persistent corneal pain after nerve injury (30), we investigated the molecular mechanism of modulation of V527M by protons. Previous studies have shown that acidic pH shifts the TRPV1 activation curve toward physiological membrane potentials, functioning as a gating modifier of the TRPV1 channel (31) similarly to heat and capsaicin (32). We performed patch-clamp experiments on HEK293 cells transiently expressing human TRPV1 to address whether V527M mutant affects gating properties of TRPV1 in response to pH. Whole-cell currents were activated using a protocol of +20 mV voltage steps from −100 to +200 mV at different values of extracellular pH (Fig. 2 *A* and *B*). For each pH, we plotted the conductance/voltage relationship (G/G_{max} vs. V) and found that increasing proton concentration induced a gradual leftward shift in the activation curve, resulting in channel activity at more physiological potentials (Fig. 2 *C* and *D*). The half-activation voltage ($V_{1/2}$) shifted with pH, for WT and mutant respectively, as follows: At pH 7.3, $V_{1/2}$ values were 130 ± 4 mV and 133 ± 6 mV; at pH 6.5, $V_{1/2}$ were 95 ± 7 mV and 87 ± 7 mV; at pH 6.0, $V_{1/2}$ were 38 ± 7 mV and 3 ± 4 mV; and at pH 5.5, $V_{1/2}$ values were 9 ± 5 mV and −19±6 mV. Overall, $V_{1/2}$ was shifted by 121 ± 5 mV for WT and 152 ± 6 mV for V527M when extracellular pH was reduced from 7.3 to 5.5 (Fig. 2*E*). These data show that protons activate TRPV1 causing a large leftward shift in the voltage dependence of activation; notably, this trend is more pronounced for the mutant, suggesting that when the pH drops, e.g., during tissue inflammation, the activity of V527M is increased at more physiological potentials compared to WT. This is a gain-of-function feature of V527M.

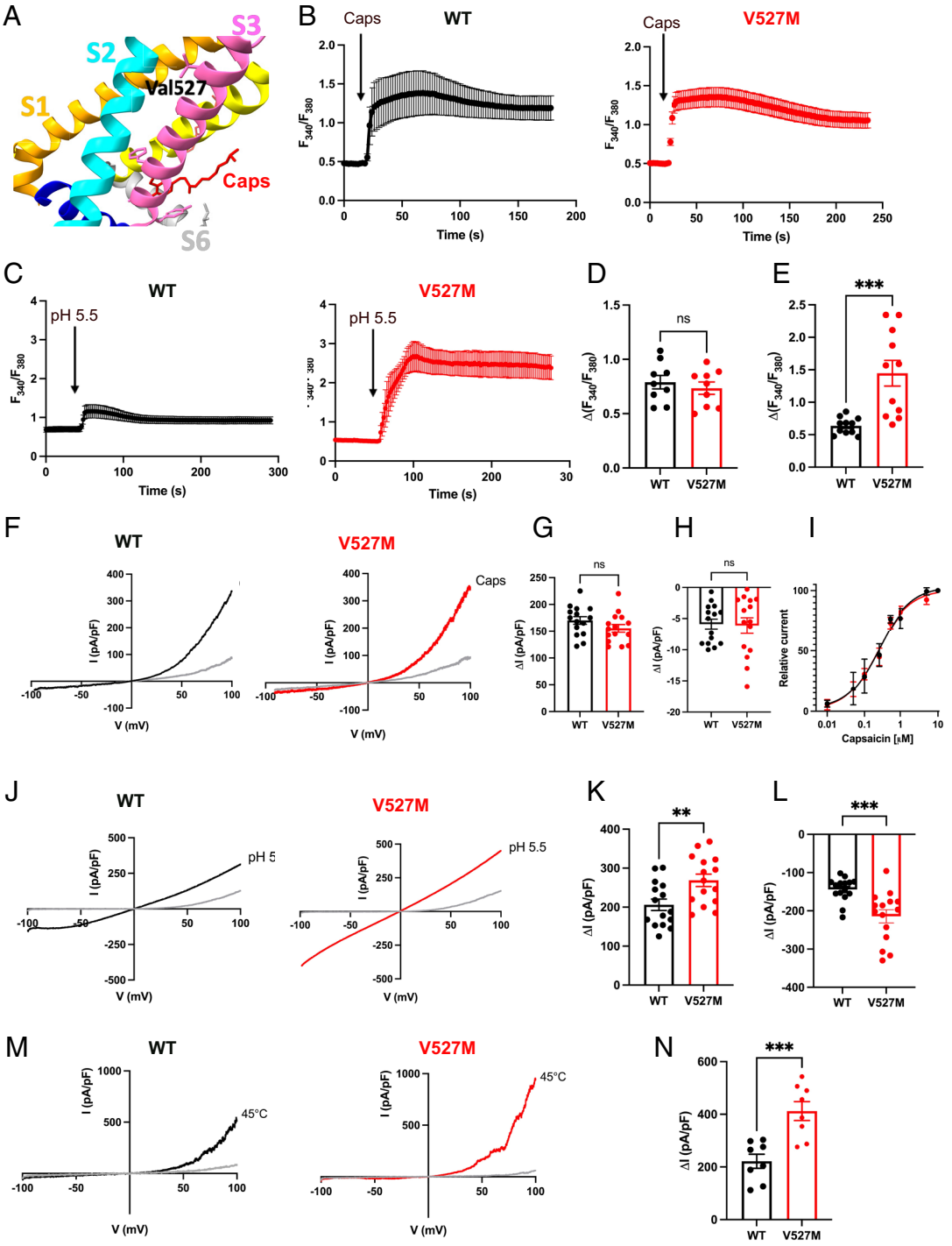

Fig. 1. V527M enhances response to acidic pH and heat. (*A*) A zoom-in view of the capsaicin binding pocket in the high-resolution structure of ratTRPV1 determined by cryo-EM (PDB7LPE) (29). A capsaicin molecule (Caps) is colored in red. The residue V527M is located in the S3 region in proximity of the vanilloid binding pocket. (*B*) Average changes in the Fura-2 ratio of HEK293 cells transfected with WT TRPV1 (black) and V527M mutant (red), in response to capsaicin (250 nM; the arrow indicates the time of addition). (*C*) Average changes in the Fura-2 ratio of HEK293 cells transfected with WT TRPV1 (black) and V527M mutant (red), in response to protons (pH5.5). (*D*) Average increase in Fura-2 ratio in response to capsaicin (unpaired Student's *t* test, n = 9 experiments, 3 transfections). (*E*) Average increase in Fura-2 ratio in response to acidic pH (***$P < 0.001$, unpaired Student's *t* test, n = 11 experiments, 3 transfections). (*F*) Representative I - V traces of whole-cell currents before (gray trace) and after (black and red traces) perfusion of capsaicin (250 nM) in HEK293 cells expressing WT TRPV1 (*Left*) or V527M mutant (*Right*). Pooled data of whole-cell current at +80 mV (*G*) and −80 mV (*H*) evoked by 250 nM capsaicin, from WT TRPV1 and V527M transfected cells. Each column represents mean ± SEM of n = 15 cells, three independent experiments (unpaired Student's *t* test). (*I*) Concentration dependence of capsaicin responses in WT TRPV1-channels and V527M mutant. Increasing concentrations of capsaicin were applied to cells expressing TRPV1-WT or TRPV1-V527M channels. Intervals between applications were 3 min. The peak amplitudes of capsaicin-activated currents were measured, normalized to the maximum response measured in each cell (which corresponds to the current elicited in the presence of 10 µM capsaicin), and plotted against capsaicin concentration. Lines represent Hill fit to the data. The values of EC50 are as follows: 267 ± 55 nM for WT and 248 ± 34 nM for V527M. The values of the Hill coefficient are as follows: 1.03 ± 0.11 for WT and 1.02 ± 0.10 for V527M. (*J*) Representative I - V traces of whole-cell currents before (gray trace) and after (black and red traces) perfusion of acidic pH (pH = 5.5) in HEK293 cells expressing WT TRPV1 (*Left*) or V527M mutant (*Right*). Pooled data of whole-cell current at +80 mV (*K*) and −80 mV (*L*) evoked by protons, from WT TRPV1 and V527M transfected cells. Each column represents mean ± SEM of n = 15 cells, three independent experiments. **$P < 0.01$ and ***$P < 0.001$ (unpaired Student's *t* test). (*M*) Representative I - V traces of whole-cell currents before (gray trace) and after (black and red traces) perfusion of preheated solution (T = 45 °C) in HEK293 cells expressing WT TRPV1 (*Left*) or V527M mutant (*Right*). (*N*) Pooled data of whole-cell current at +80 mV evoked by heat stimulus. ***$P < 0.001$ (n = 8 cells, unpaired Student's *t* test).

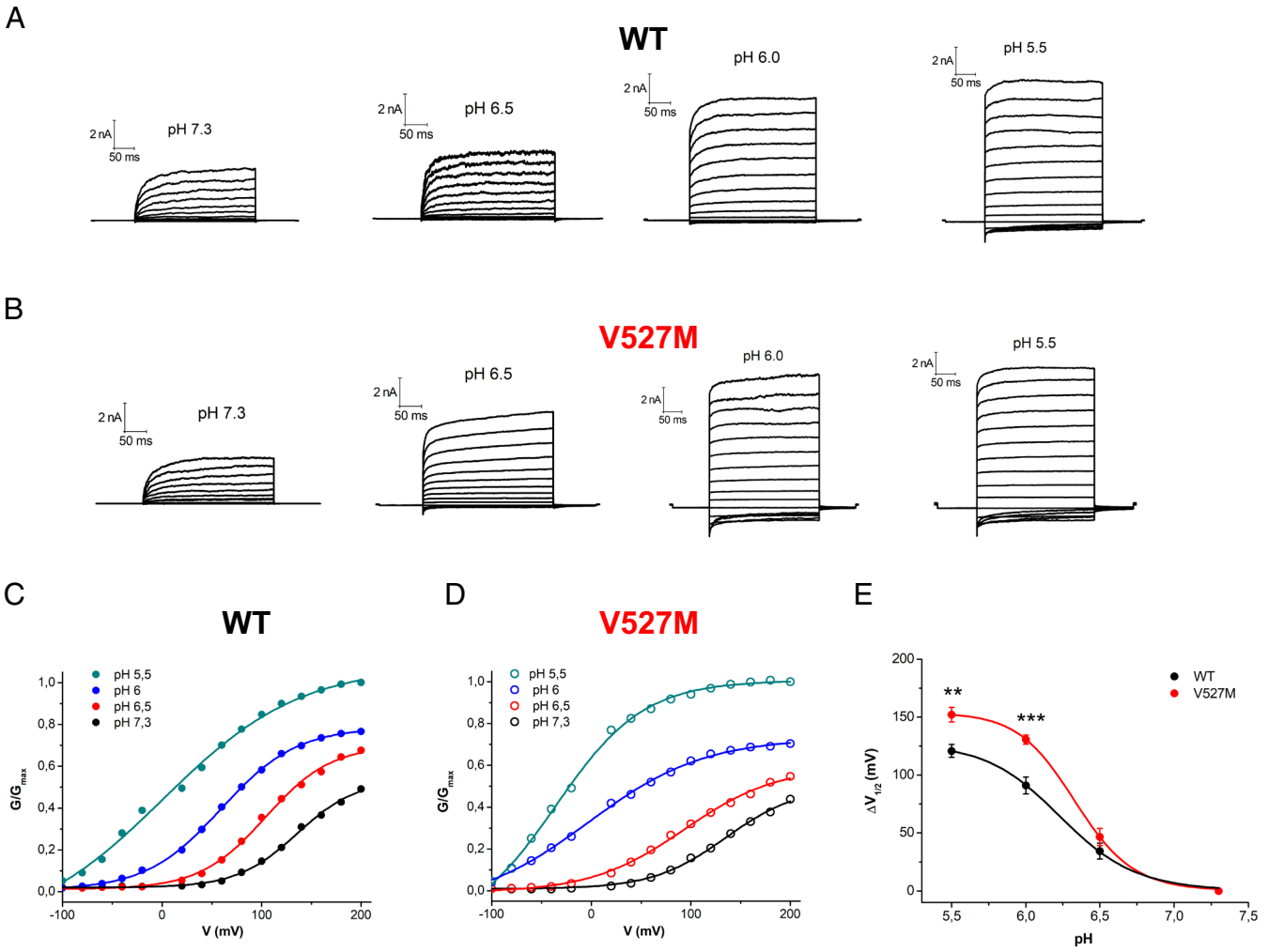

Fig. 2. V527M affects pH-mediated channel gating. Representative whole-cell current traces through WT TRPV1 (*A*) and V527M (*B*) transfected cells at the indicated pH, in response to 20 mV-voltage steps from −100 mV to +200 mV. (*C*) Normalized steady-state maximal conductance curves at different pH values, obtained from current traces shown in *A*, recorded in HEK293 cells expressing WT TRPV1. (*D*) Normalized steady-state maximal conductance curves at different pH values, obtained from current traces shown in *B*, recorded in HEK293 cells expressing V527M. Lines represent Boltzmann fit to the data. (*E*) $\Delta V_{1/2}$ as a function of pH for WT TRPV1, and V527M. Lines represent Hill fit to the data. Error bars represent SEM (**$P < 0.01$ and ***$P < 0.001$, 2-way ANOVA with the Bonferroni post hoc test, n = 10 cells).

V527M Increases Trigeminal Ganglia (TG) Neuronal Excitability. To address whether V527M expression alters excitability of sensory neurons innervating the eye, current-clamp recordings were performed on cultured TG neurons transiently transfected with WT and V527M TRPV1 plasmids.

TRPV1 plasmids were transfected in TG neurons obtained from WT rat pups, with an efficiency of ~20% as previously reported for primary sensory neurons (33). All experiments were performed on small-diameter sensory neurons (diameter < 25 µm) expressing GFP-tagged WT TRPV1 and V527M. Representative action potential traces from WT and V527M TG neurons in response to depolarizing current steps show that an action potential was elicited at a threshold of 200 pA for WT TRPV1 and 80 pA for V527M expressing neurons (Fig. 3*A*). While the basal intracellular Ca^{2+}, as assessed by initial Fura-2 signal ratios, was not significantly different between WT and V527M transfected TG neurons (Fig. 3*B*), the resting membrane potential was significantly depolarized in V527M neurons compared to WT neurons (WT, –50.8 ± 1.4 mV, n = 22; V527M, –44.3 ± 1.5 mV, n = 18; Fig. 3*C*). In addition, the V527M mutation almost doubled the evoked firing activity in TG neurons, expressed as the maximum average number of action potentials in response to a 750 pA stimulus of 1 s duration (WT, 5 ± 1, n = 22; V527M, 10 ± 1, n = 18; Fig. 3*D*). The mean current threshold for action potential firing in V527M transfected neurons was significantly lower compared to WT transfected TG neurons (WT, 133 ± 13 pA, n = 22; V527M, 64 ± 15 pA, n = 18; Fig. 3*E*). Finally, Ca^{2+} imaging experiments were performed to address whether response to protons was enhanced in TG neurons expressing the mutant. Our results show that the amplitude of Ca^{2+} signals generated by TRPV1 activation in response to protons (pH 5.5.) was significantly increased in neurons expressing V527M compared with WT neurons, confirming that V527M is a gain-of-function mutation for acidic pH leading to increased neuronal activity under acidic conditions (Fig. 3 *F* and *G*).

V527M Affects Capsaicin-Induced Desensitization. Activation of TRPV1 by agonists, e.g., capsaicin, is followed by desensitization and tachyphylaxis of nociceptors, via a process that dampens the ability of the receptor to respond to further application of capsaicin or other noxious stimuli. The desensitization of TRPV1 is a Ca^{2+}-dependent process and involves different intracellular signaling pathways (34). The classical model of TRPV1 desensitization holds that the fast component of desensitization is triggered by the Ca^{2+}-dependent binding of calmodulin to the channel, while the second phase of desensitization involves Ca^{2+}-dependent

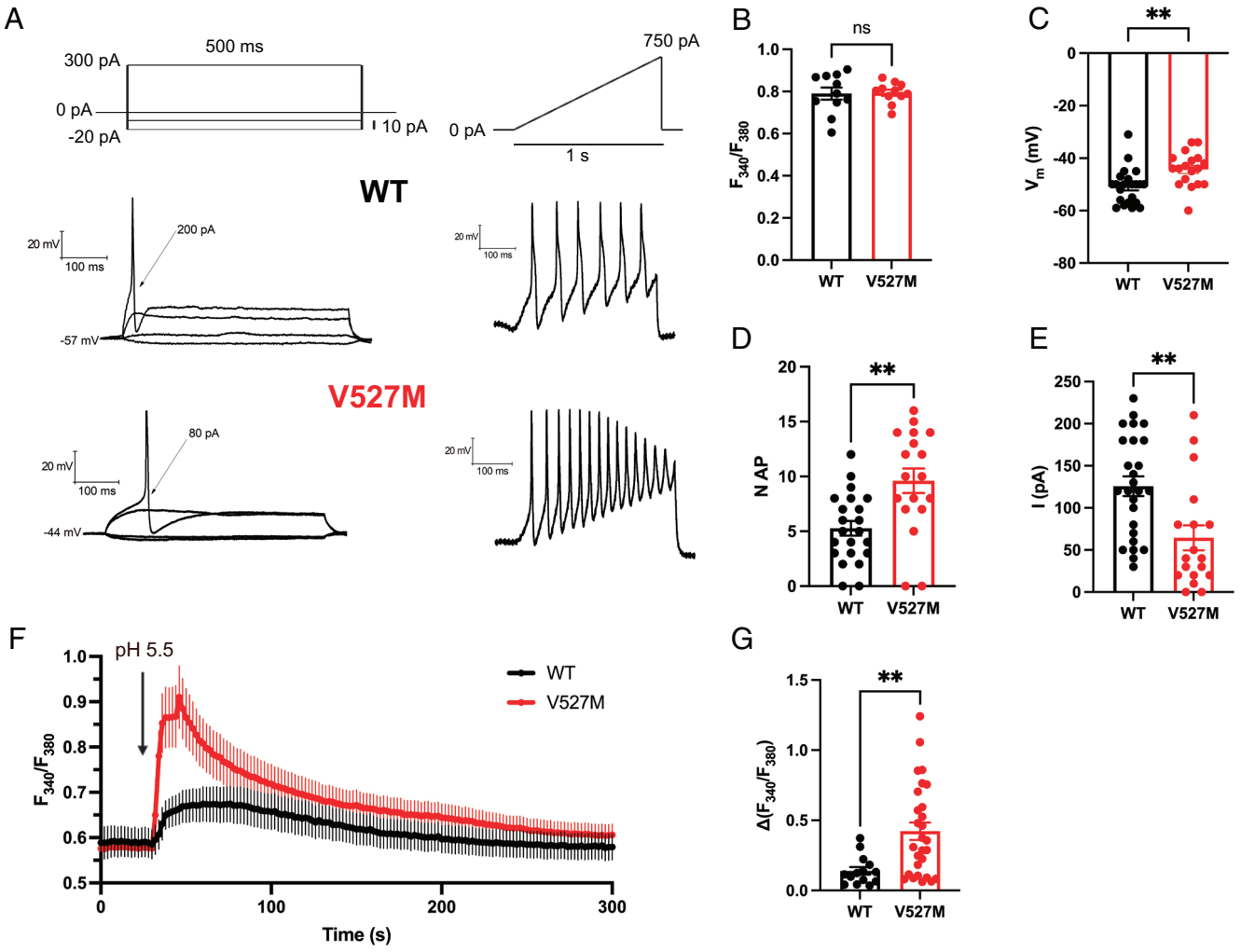

Fig. 3. V527M increases TG neuronal excitability. (*A*) Representative traces from a WT TRPV1 and V527M transfected TG neuron, showing current threshold (*Left*) and action potential frequency (*Right*) in response to current stimuli shown on *Top*. Arrows indicate the current amplitude used to elicit the labeled response (200 pA for WT and 80 pA for V527M, respectively). Comparison of basal Ca^{2+} concentration (n = 11 coverslips) (*B*), resting membrane potential (*C*), maximal number of action potentials evoked in response to external current stimuli of 1 s, up to 750 pA (*D*), and current threshold (*E*) in WT (n = 22) and V527M (n = 18) transfected neurons. Each column represents mean ± SEM. $^{**}P < 0.01$ (unpaired Student's *t* test). (*F*) Average changes in the Fura-2 ratio of TG neurons transfected with WT TRPV1 (black) and V527M mutant (red), in response to protons (pH 5.5); the arrow indicates the time of addition of acidic pH solution. (*G*) Average increase in Fura-2 ratio in response to acidic pH ($^{**}P < 0.01$, unpaired Student's *t* test, n = 17 for WT, 30 for V527M).

phosphorylation/dephosphorylation processes that modulate endocytosis and degradation of TRPV1 in nociceptors via a clathrin-independent pathway (35, 36).

To test the effect of the V527M mutation on agonist-induced TRPV1 tachyphylaxis, we performed patch-clamp recordings and measured the response to consecutive applications of 250 nM capsaicin (Fig. 4*A*). As expected from the classical behavior of TRPV1 (34), we found that in WT TRPV1 channels the second response to capsaicin was reduced to about half of the first response (43 ± 4%, Fig. 4*C*). We then tested the capsaicin-induced desensitization of V527M under the same conditions (perfusion of 250 nM capsaicin, 2 mM Ca^{2+} in the extracellular solution) (Fig. 4*B*) and found that the ratio of the second to the first response of V527M to capsaicin was 82 ± 6% (Fig. 4*C*), which was significantly higher than that of WT. Moreover, the deactivation rate was markedly slowed down in V527M. At +80 mV, the desensitization time constant was 7.8 ± 2.3 s for WT and 25.0 ± 5.3 s for V527M (Fig. 4*D*). Overall, these data indicate that V527M affects the deactivation gating process, by reducing capsaicin-induced desensitization and tachyphylaxis, and thus demonstrate another pro-excitatory effect on the mutant TRPV1.

To characterize the neuronal response to capsaicin and test whether V527M also affects desensitization of nociceptors, we performed patch-clamp recordings in acutely dissociated trigeminal neurons transfected with WT and V527M hTRPV1. As shown in Fig. 4*E*, 250 nM capsaicin exposure of TG neurons expressing TRPV1 WT evoked robust depolarization and a series of spikes, followed by immediate depolarization blockade and acute desensitization as the membrane potential recovered quickly to resting membrane potential values, as previously described (37). In TG neurons expressing V527M the same stimulus with the same duration (250 nM capsaicin for 15 s) produced a significantly longer depolarization stimulus compared with TG neurons expressing WT and a slower acute desensitization induced by capsaicin (Fig. 4*E*). To describe and compare acute desensitization quantitatively for TG neurons expressing TRPV1-WT and V527M, we measured the areas under the current curves from the beginning of the experiment until the restoration to resting membrane potential. These experiments showed that the mean value of the area relative to the mutant was significantly higher than WT (850 ± 253 mV*s for WT; 2,787 ± 164 mV*s for V527M, suggesting that V527M

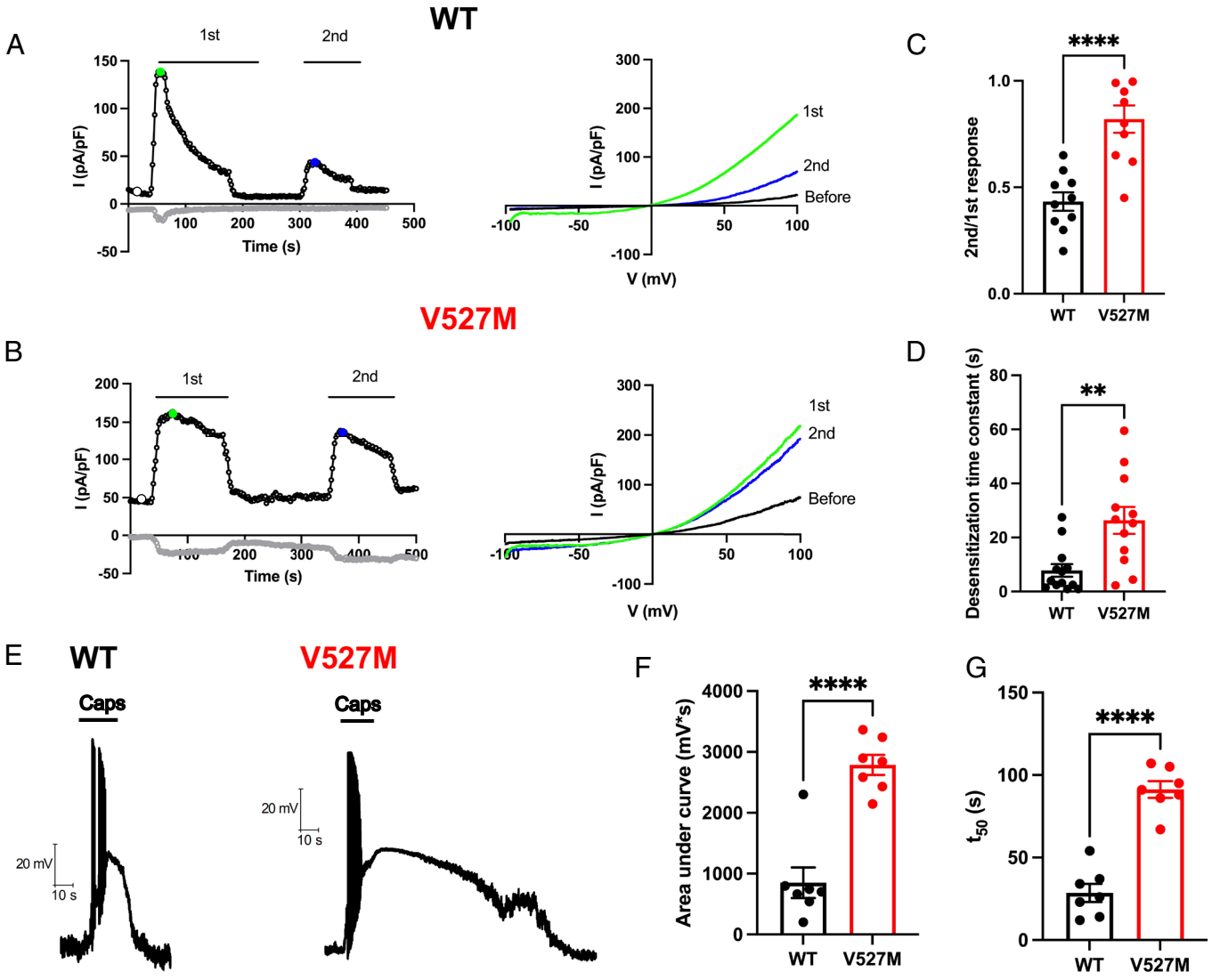

Fig. 4. V527M affects capsaicin-induced desensitization. Representative time courses (*Left*) and I to V traces (*Right*) of development of TRPV1 current in response to two consecutive applications of 250 nM capsaicin are shown for WT (*A*) and V527M (*B*). (*C*) Ratios of second response/first response at +80 mV after two consecutive applications of capsaicin. (*D*) Summary of desensitization single exponential time constant. Data were expressed as mean ± SEM; n = 13 cells for WT and n = 12 cells for V527M. $^{**}P < 0.01$ (unpaired Student's *t* test). (*E*) Representative current-clamp recordings (I = 0) from a TRPV1 WT and V527M transfected TG neuron in response to capsaicin (250 nM) that was applied for 15 s. (*F*) Areas under the curves of current-clamp recordings (I = 0) from TRPV1 WT and V527M transfected TG neurons in response to capsaicin (250 nM). Each column represents mean ± SEM. $^{****}P < 0.0001$ (unpaired Student's *t* test, n = 7). (*G*) Time to half maximum current (t_{50}) in response to 250 nM capsaicin. Each column represents mean ± SEM. $^{****}P < 0.0001$ (unpaired Student's *t* test, n = 7).

showed significantly reduced acute desensitization compared with WT TG neurons (Fig. 4*F*). Finally, we compared the desensitization rate of capsaicin-activated current represented by time to half maximum current ($t_{50;}$ the time taken for the current to decrease to 50% of its level after capsaicin application) measured during the acute desensitization phase: We found that the t_{50} was markedly increased in V527M-expressing TG neurons, confirming that V527M significantly slowed-down capsaicin-induced desensitization in nociceptors (Fig. 4*G*).

V527M Increases Capsaicin Sensitization by BK and Enhances 12-HETE Activation. Inflammation of the ocular surface after nerve injury promotes the release of a large variety of chemicals by local cells (epithelium cells, fibroblasts, mast cells, neutrophils, monocytes, and platelets), including protons and BK (38).

Previous studies have shown that BK potentiates TRPV1 channel activity leading to nociceptor hyperexcitability and NeP (27, 39–42). To assess whether V257M mutation affects BK potentiation and sensitization of the TRPV1 channel, we performed Ca^{2+} imaging experiments on TG neurons expressing WT and V527M hTRPV1, respectively. Application of BK resulted in a small and not significantly different increment of intracellular Ca^{2+} in TG neurons expressing WT and V527M TRPV1 channels (Fig. 5 *A* and *B*). However, a subsequent pulse of capsaicin, the TRPV1 agonist, produced a significantly higher response in V527M-transfected neurons compared with WT. Specifically, the response to capsaicin after BK administration was 1.5 ± 0.2-fold greater in the mutant, consistent with a stronger enhancement of the BK-induced V527M response than in WT (Fig. 5 *A* and *C*).

To gain a deeper understanding of the molecular mechanism underlying the increased BK sensitization in V527M mutant, we performed Ca^{2+} imaging experiments in the presence of endogenous lipids that are known to activate TRPV1 channels and are mainly produced during inflammation (20, 43–46). We focused on the endovanilloid lipid 12-HETE, which is a product of AA metabolism by lipoxygenases (LOX), downstream of the Gq/G protein-coupled receptors (GPCR) pathway (47–50) and is known to be released in the cornea during inflammation and after tissue damage (51–58).

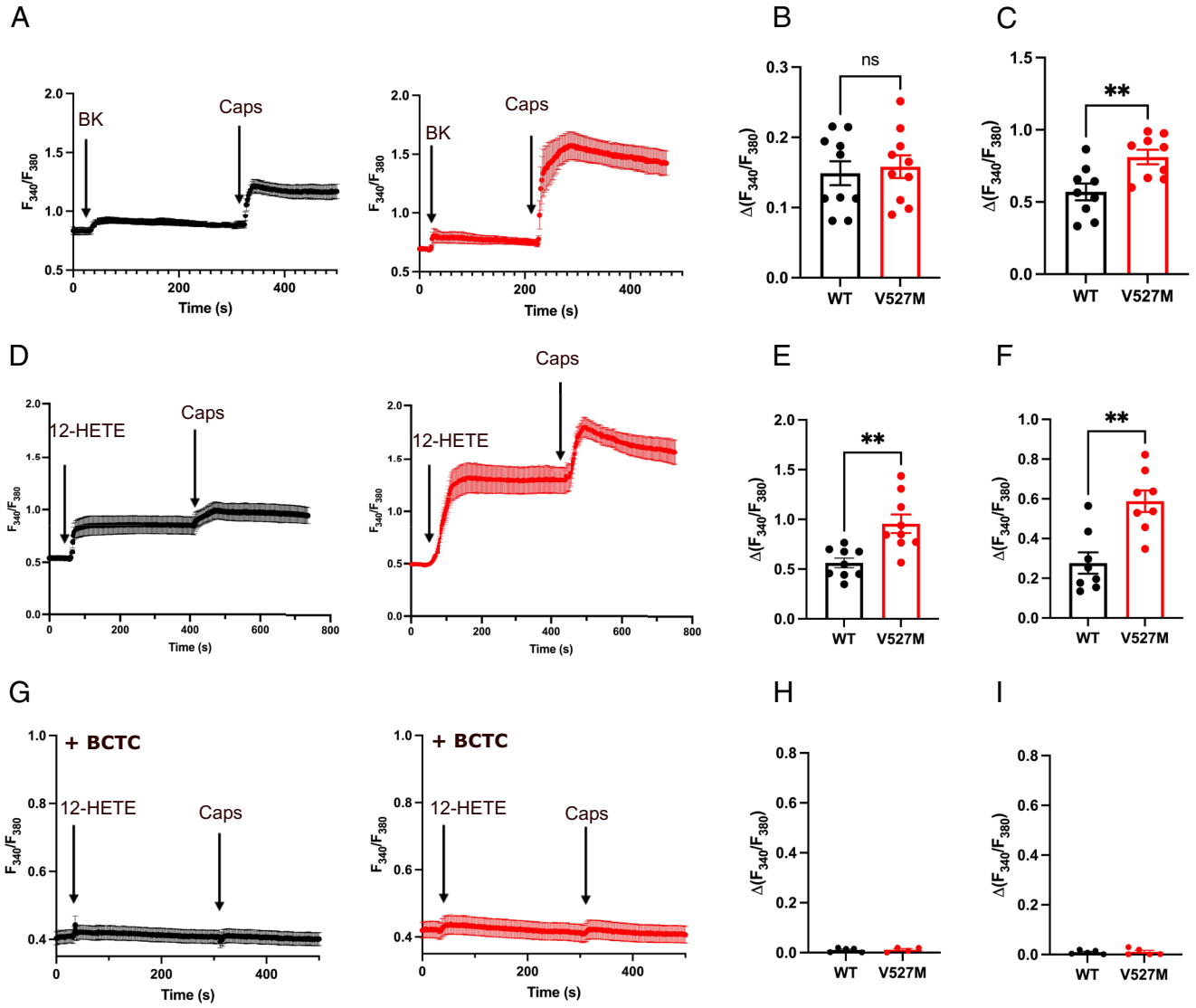

Fig. 5. V527M increases capsaicin sensitization by BK and enhances 12-HETE activation. (*A*) Average changes in the Fura-2 ratio of TG neurons transfected with WT TRPV1 (black) and V527M mutant (red), in response to BK (500 nM) and capsaicin (Caps, 250 nM); the arrow indicates the time of addition. Average increase in Fura-2 ratio in response to BK (*B*) and capsaicin (*C*) (**$P < 0.01$, unpaired Student's *t* test, n = 9 experiments, 3 transfections). (*D*) Representative average changes in Fura-2 ratio in WT (black) and V257M (red) transfected TG neurons in response to 12-HETE (1 μM) and capsaicin (Caps, 250 nM). Average increase in Fura-2 ratio in response to 12-HETE (*E*) and capsaicin (*F*) (**$P < 0.01$, unpaired Student's *t* test, n = 8 experiments, 3 transfections). (*G*) Representative average changes in Fura-2 ratio in WT (black) and V257M (red) transfected TG neurons in response to 12-HETE (1 μM) and capsaicin (250 nM), in the presence of 100 nM BCTC. Average increase in Fura-2 ratio in response to 12-HETE (*H*) and capsaicin (*I*).

These experiments showed that the response to 12-HETE was significantly increased in V527M-transfected neurons compared with WT (Fig. 5 *D* and *E*). In addition, we observed increased capsaicin sensitization for the mutant channel after 12-HETE application compared with WT (Fig. 5 *D* and *F*), similar to what was observed after BK application, suggesting that the BK-induced increased sensitization of V527M may be linked to the increased affinity of the mutant for the endogenous vanilloid ligand 12-HETE. As expected, in the presence of the TRPV1 antagonist BCTC (100 nM) the effect of 12-HETE and capsaicin was completely abolished (Fig. 5 *G–I*), pointing to a direct binding between TRPV1 and 12-HETE.

Discussion

PRK and LASIK are common surgical techniques to correct refractive error. These procedures provide a human model in which there is reproducible injury into trigeminal afferents. In LASIK, the distal axons of trigeminal ganglion sensory neurons within the cornea are transected; in PRK, nerves in the subbasal plexus and some stromal processes are ablated. In a small fraction of patients, these procedures are associated with persistent postoperative pain, called corneal neuralgia (16).

Consistent with other models of pain related to nerve injury, corneal neuralgia is attributed to an abnormal hyperexcitability of nociceptors and peripheral sensitization, plausibly with a contribution by altered activity of ion channels involved in sensory transduction (59).

A recent study investigated the contribution of genomic factors to corneal neuralgia after photorefractive surgery (17), revealing, through WES analysis, several variants in electrogenisome-related ion channel and collagen gene panels. A large number of these variants belong to TRP channels, that are widely expressed in sensory nerve terminals innervating the eye (60).

The terminal branches of the ophthalmic nerve exhibit specific sensitivities to distinct stimuli due to the selective expression of ion channels, mainly TRP channels, in the cornea: About 40% of ocular TG neurons are polymodal nociceptors, sensitive to heat, acidity,

and chemicals due to the presence of TRPA1 and TRPV1 channels and acid-sensing ion channels (ASIC1 and 3) (61); 50% are cold thermoreceptors due to the expression of TRPM8 channel (62), and 10% are mechanoreceptors due to the presence of Piezo-2 mechanosensitive channel (63). In addition, TG neurons express voltage-gated sodium (Na_V), potassium (K_V), and calcium (Ca_V) channels and ligand-gated channels, such as hyperpolarization-activated cyclic nucleotide-gated channels, which shape neuronal excitability and modulate frequency and firing pattern of nerve impulses generated at peripheral sensory terminals in ocular tissues (64). Dysregulation of these channels following LASIK or PRK could contribute to corneal neuralgia.

Here, we analyzed a mutation of the TRPV1 channel, V527M, found in a 49-y-old woman who developed persistent corneal pain 1 mo after PRK enhancement of LASIK surgery performed at age 30. The purpose of the study was to understand whether and how the V527M mutation predisposes the carrier to the onset of corneal neuralgia. The V527M variant (rs201666201) in the gnomAD (v4.1.0) database is 23/15930.

First, we found that V527M mutation confers a gain-of-function attribute on the channel in acidic pH. Tissue acidosis is a common phenomenon found in inflammation, in lesions or incisions, and even in malignant tumors. High local proton concentrations in inflamed tissues can excite and sensitize rat skin nociceptors (65, 66) and can cause sustained pain in experimental acidosis of human skin and cornea (67–69). In a rat model of postoperative pain, incision of the hind paw caused local decrease in pH that activates ASIC and TRPV1 channels (70). The opening of these channels induced peripheral sensitizations that was involved in the development and maintenance of chronic surgical pain (71).

Similarly, in the eye, protons are released from damaged cells in the ocular surface during inflammation, after tissue injury, or during chronic conditions (72). Our data show that TG neurons expressing V527M generate higher Ca^{2+} influx in response to acidic pH, suggesting that the peripheral corneal terminals expressing V527M are more sensitive to tissue acidosis. We therefore hypothesize that in the patient carrying the V527M mutation, protons released during corneal inflammation generate increased depolarization in trigeminal neurons, inducing peripheral sensitization of these afferents and leading to NeP.

However, the TRPV1 channel is known to be activated by strong acidification, with a pH threshold for acid-induced activation between 5.9 (at 22 °C) and 6.4 (at 37 °C) (26), so the channel is likely to be activated at pH < 6 at physiological temperatures in the cornea. These data suggest that the acidification that occurs during ocular inflammation is most likely not sufficient to activate TRPV1 directly; instead, it may enhance its response to other TRPV1 agonists, e.g., heat, voltage, or inflammatory agents, thus intensifying painful sensations. Interestingly, our data show that V527M affects pH-mediated channel gating, causing a leftward shift in the voltage dependence of activation at acidic pH. This suggests that when pH drops, for example under inflammatory conditions, the activity of the mutant is greater than WT at more physiological potentials and less acidic pH. Moreover, the proton sensitivity of TRPV1 can be further enhanced by inflammatory mediators (e.g., BK, AA metabolites, lactate, or hypertonicity) which shift acid activation toward less acidic pH values. These inflammatory mediators are commonly found in the cornea after tissue damage (38). Notably, it has been previously shown that the combination of inflammatory mediators (BK, 5-HT, PGE2, and histamine) in acid solution (pH 6.1) can excite and sensitize rat skin nociceptors (64).

Our results show that V527M enhances BK-induced sensitization of TRPV1 channels. We found that the response to capsaicin after BK administration was 1.5 ± 0.2-fold greater in trigeminal neurons expressing V527M compared to TG neurons expressing WT TRPV1, consistent with a stronger potentiation of the BK-induced V527M response in trigeminal neurons that carry the mutant channel. Hence, we can speculate that in the carrier of V527M mutation, the combination of BK and moderate acidification associated with corneal inflammation may sensitize nociceptors and cause NeP.

It has been previously demonstrated that TRPV1 is activated, via GPCRs, by inflammatory compounds, e.g., BK, histamine, prostaglandin, and serotonin, that cause sensitization of peripheral nociceptors during thermal and inflammatory hyperalgesia (27, 39–42). It has been also shown that BK sensitizes TRPV1 through protein kinase C (PKC-) and protein kinase A (PKA)-mediated phosphorylation of specific intracellular Ser/Thr residues of the receptor, resulting in increased channel activity (40–42, 72–74).

Endogenous lipids such as anandamide (44) and lipoxygenase-derived metabolites of the membrane phospholipid AA, e.g., hydroperoxyeicosatetraenoic acid (HPETE) and HETE (48–50), have been suggested as possible mediators of GPCR-activation of TRPV1.

We found that the response to the endovanilloid lipid 12-HETE, produced during corneal pain, was significantly increased in V527M-transfected neurons compared with WT and was completely abolished in the presence of the TRPV1 antagonist BCTC. Moreover, the response to capsaicin after perfusion of 12-HETE was significantly enhanced in V527M-transfected neurons, thereby eliciting in the mutant the same effect as BK-sensitization. These results may support the idea that 12-HETE is the lipid mediator responsible for the different effect of BK in the V527M-tranfected TG neurons compared to WT TG neurons.

It remains unclear whether endovanilloids produced by LOX metabolism downstream of Gq/GPCR signaling bind directly to the vanilloid binding site or whether their activity depends on phosphorylation of TRPV1 by PKC.

12- and 15-(S)-hydroperoxyeicosatetraenoic acids have previously been shown to activate the TRPV1 channel by direct binding (48). 20-HETE, also derived from AA, activates and sensitizes TRPV1 in humans and mice (75) and the activation involves the Ser502 residue, which is critical for the functional phosphorylation of TRPV1 (76, 77). Recently, it has also been proposed that endovanilloids produced by LOX metabolism promote TRPV1 activation through the combined activity of two different mechanisms: direct binding of TRPV1 through the endovanilloid binding site and sensitization of TRPV1 through PKC (50).

The V527 residue is located near the vanilloid binding pocket (Fig. 1*A*). This might suggest an involvement of V527 in direct binding to 12-HETE. However, the increase of BK-induced sensitization of V527M also seems to indicate that the mutation leads to the modification of channel gating properties through an enhanced phosphorylation of TRPV1. Therefore, we cannot rule out the possibility that a combination of both mechanisms, i.e., direct binding of TRPV1 through the endovanilloid binding site and sensitization of TRPV1 through PKC, may explain the increased activation of V527M by 12-HETE and the increased sensitization of V527M by BK.

Finally, the V527M mutation decreases capsaicin-induced desensitization. The reduced desensitization represents a gain-of-function because the decreased extent of desensitization would increase subsequent TRPV1 signaling in response to repeated application of agonists. The decrease of desensitization may influence nociceptor excitability by promoting a small but continuous accumulation of Ca^{2+} during repeated agonist application, which might lead to hyperexcitability and the onset of NeP in neurons expressing V527M.

This case is notable in that pain did not develop after the first surgery in the presence of the TRPV1 V527M mutation.

A plausible explanation is that "two hits" are required. One possibility is that the first surgery resulted in microglial priming (78). Within this schema the second hit, PRK enhancement, caused enhanced pain intensity and duration mediated by the V527M mutation with its altered integration of inflammatory signals. The eyes are subject to persistent postoperative pain much like other organs and tissues and insights garnered from this case might help in the prevention or treatment of other postoperative pain syndromes (79). Although genetic screening is not yet mainstream for LASIK or other elective refractive surgery, it is current practice to screen out patients with uncontrolled autoimmune or immune-mediated disease or uncontrolled mental illness, including anxiety or depression, because of association with problems such as poor healing, reduced satisfaction, and persistent postoperative pain (80).

Ghovanloo et al. (81) studied a $Na_V1.7$ mutation (P610T) found in two siblings with persistent ocular pain after corneal refractive surgery and found that it impaired channel slow inactivation and conferred hyperexcitability in trigeminal ganglion neurons consistent with NeP. We cannot exclude a contribution of inflammatory pain in the present case but suggest that if inflammatory mechanisms contributed to pain, this occurred following corneal axonal injury in the context of a TRPV1 mutation that increases excitability of trigeminal ganglion neurons. Additionally, patients with persistent postoperative pain after refractive surgery typically have no clinical evidence of tissue injury or inflammation on standard slit lamp examination of the surgical field. The cornea being transparent and at the body surface is special in allowing opportunity for such microscopic examination of a postoperative field. The more recent use of In vivo confocal microscopy of the cornea in such patients shows reduced nerve density, increased nerve tortuosity, microneuromas, as well as dendritic cells, all of which suggest neuropathic basis with inflammatory components (82).

In the aggregate, our results suggest a mechanism by which this TRPV1 mutation contributes to corneal neuralgia after refractive surgery. It also represents an example of a mutation that causes susceptibility to NeP by increasing the excitability of trigeminal ganglion neurons in resting conditions and, at the same time, integrates multiple inflammatory signals, including increased sensitivity to BK and protons released after trigeminal nerve injury, into the pain-producing cascade.

Methods

Plasmid, Cell Culture, and Transfection. Patch-clamp studies were carried out in HEK 293 cells transiently transfected with plasmids encoding human WT TRPV1 and V527M mutant channels. For heterologous expression, cells were plated in 6-well cell culture dishes with 2-mL growth medium (DMEM, 10% FBS, 2 mM L-glutamine, 2 U/mL penicillin, and 2 mg/mL streptomycin) 24 h before transfection. Transfection was performed using Lipofectamine LTX reagent (Invitrogen) as described previously (11, 12). Cells were incubated at 32 °C after transfection with WT and mutant to enhance expression of TRPV1 channels at the membrane. The WT TRPV1 plasmid was obtained from GenScript, in which the insert was cloned in-frame with 2A-GFP at the C terminus of the channel in the vector pcDNA3.1. The single TRPV1-2AGFP transcript is translated into the separate channel protein and the transfection marker GFP (83, 84). The V527M mutation was introduced into the TRPV1 channel using QuikChange Lightning site-directed mutagenesis (Agilent Technologies).

Isolation, Culture, and Transfection of Rat TG Neurons. For each transfection, TGs from three rat pups (1 to 3 d) were dissected and digested with 12.5 mg/mL collagenase and 3 mg/mL dispase for 35 min at 37 °C and then triturated. The resulting cell suspension was filtered through a 100 μm cell strainer (VWR) to remove debris. Transfection of TG neurons was performed as previously described (33). TG neurons isolated were resuspended with 100 μL of Nucleofector solution (Mouse Neuron NucleofectorTM Kit, VPG-1001, Lonza) and mixed with DNA (10 μg of plasmids). TG neurons were transfected using the Nucleofector 2b Electroporator (Lonza, Walkersville, MD) using the protocol G-013. After electroporation, 500 μL of calcium-free Dulbecco's Modified Eagle Medium (DMEM) (37 °C) was added to the cell mixture and incubated for 5 min with 5% CO_2 at 37 °C to allow neurons to recover. Neurons were cultured in complete medium containing DMEM/F12, 10% of fetal bovine serum (FBS), and 1% of penicillin–streptomycin on coverslips coated with 0.1 mg/mL of Poly-L-lysine and 10 μg/mL of laminin and incubated with 5% CO_2 at 37 °C. Imaging and patch clamp experiments were performed 24 to 48 h after culture.

Electrophysiology. Patch-clamp recordings of HEK293 cells were carried out at room temperature, using an EPC-9 amplifier (HEKA Elektronik, Lambrecht, Germany) controlled by PatchMaster software (HEKA Elektronik, Lambrecht, Germany). Patch-clamp electrodes were pulled and fire polished to 4.0 ± 0.5 MΩ resistance when filled with intracellular solution, using a DMZ-Universal Puller (Zeitz Instruments, Munich, Germany). An AgCl wire was used as a reference electrode. To elicit I –V whole-cell currents, repetitive 400 ms voltage ramps (at 2 s intervals) from −100 mV to +100 mV were applied, from a holding potential of 0 mV. Currents were sampled at 20 kHz and digitally filtered at 2.9 kHz. For statistical analysis, the currents were normalized to cell capacitance. Solutions were applied to cells via a custom-built gravity-fed perfusion system, connected by a 5-way manifold, to a RC25 perfusion chamber (Warner Instruments). For patch-clamp experiments involving the activation of TRPV1 by heat, the temperature was controlled with a Peltier PTC-20 temperature control system (NPI Electronic).

For voltage-clamp recordings in HEK cells, the standard extracellular solution had the following composition (in mM): 140 NaCl, 5 KCl, 2 $CaCl_2$, 1 $MgCl_2$, 10 glucose, and 10 4-(2-Hydroxyethyl)-1-piperazine ethanesulfonic acid (HEPES), buffered at pH 7.4 with NaOH. The osmolarity of the extracellular solution was 315 ± 5 mOsm. The intracellular solution had the following composition (in mM): 140 CsCl, 0.08 $CaCl_2$, 10 EGTA, and 10 HEPES, adjusted to pH 7.2 with CsOH (290 ± 5 mOsm). For current clamp recordings in isolated TG neurons, the extracellular composition had the following composition (in mM): 154 NaCl, 3 KCl, 1 $CaCl_2$, 1 $MgCl_2$, and 10 HEPES adjusted to pH 7.4 with NaOH (350 ± 5 mOsm). The intracellular solution had the following composition (in mM): 137.5 K-Glutamate, 11 NaCl, 11 EGTA, 11 HEPES, and 11 glucose adjusted to pH 7.2 with KOH (310 ± 5 mOsm).

Ca^{2+} Imaging. Loading of HEK293 cells and TG neurons with Fura-2 AM was achieved at 37 °C in Krebs medium with fluorophore concentration of 5 μM and 0.01% pluronic acid F-127 for 1 h (Fura2-AM). $[Ca^{2+}]_i$ was measured in 10 to 15 individual cells for each experiment using alternative excitation (0.5 Hz) at 340 and 380 nm using a Lambda DG-4 Ultra High Speed Wavelength Switcher (Sutter Instrument, Novato, CA, USA). Images were acquired with a Zeiss Axiocam camera coupled to a 510-nm emission filter and analyzed with Axiovision software. Ca^{2+} imaging experiments were performed in the following solution: NaCl 140 mM, KCl 5 mM, $CaCl_2$ 2 mM, $MgCl_2$ 1 mM, HEPES 10 mM, and glucose 10 mM, pH 7.4. The extracellular solution pH was 5.0, 5.5, or 6.5 in the experiments where V527M response to acidic pH was tested.

Data Analysis. Current recordings were analyzed using Clampfit 10.7. OriginPro 2016 and GraphPad software were used for statistical analysis and data display. Pooled data of current and imaging recordings are presented as mean ± SEM. Significance was established at $P < 0.05$. N is the number of "cells" used for electrophysiological experiments or the number of "coverslips" (>10 cells) used for imaging experiments.

To analyze the effects of the mutation V527M on the pH-mediated channel gating of TRPV1, we applied voltage steps of 20 mV from –100 to +200 mV. G/G_{max} – V relationship data were fitted using a Boltzmann function, and pH–response relationships were fitted using a Hill equation.

Data, Materials, and Software Availability. All study data are included in the main text.

ACKNOWLEDGMENTS. We thank Prof. Carlos Belmonte for the valuable advice and fruitful discussions on corneal neuralgia and Fadia B. Dib-Hajj for technical assistance. Work toward this study in the laboratory of S.D.-H. and S.G.W. was supported by Center Grant I50Rx002999 from the Department of Veterans Affairs and by funding from the Paralyzed Veterans of America and the Flaherty endowment to Yale. The Center for Neuroscience and Regeneration Research is a Collaboration of The Paralyzed Veterans of America and Yale University. Work for this study at the University of Louvain was supported by the Belgian Fund for Scientific Research (FNRS, grant PDR–T.0089.22 to P.G. and grant MIS–F.4028.24 to R.G.).

1. IASP, IASP taxonomy. https://www.iasp-pain.org/terminology?navItemNumber=576. Accessed 2 September 2019.
2. S. N. Raja *et al.*, The revised International Association for the Study of Pain definition of pain: Concepts, challenges, and compromises. *Pain* **161**, 1976–1982 (2020).
3. N. B. Finnerup, R. Kuner, T. S. Jensen, Neuropathic pain: From mechanisms to treatment. *Physiol. Rev.* **101**, 259–301 (2021).
4. S. N. Raja, M. Ringkamp, Y. Guan, J. N. Campbell, Peripheral neuronal hyperexcitability: The "low-hanging" target for safe therapeutic strategies in neuropathic pain. *Pain* **161**, S14–S26 (2020).
5. K. Zorina-Lichtenwalter, C. B. Meloto, S. Khoury, L. Diatchenko, Genetic predictors of human chronic pain conditions. *Neuroscience* **338**, 36–62 (2016).
6. L. J. Hocking *et al.*, Heritability of chronic pain in 2195 extended families. *Eur. J. Pain* **16**, 1053–1063 (2012).
7. S. G. Waxman, Polymorphisms in ion channel genes: Emerging roles in pain. *Brain* **133**, 2514–2518 (2010).
8. M. Calvo *et al.*, The genetics of neuropathic pain from model organisms to clinical application. *Neuron* **104**, 637–653 (2019).
9. G. Cruccu, G. Di Stefano, A. Truini, Trigeminal neuralgia. *N. Engl. J. Med.* **383**, 754–762 (2020).
10. G. Cruccu *et al.*, AAN-EFNS guidelines on trigeminal neuralgia management. *Eur. J. Neurol.* **15**, 1013–1028 (2008).
11. R. Gualdani *et al.*, Trigeminal neuralgia TRPM8 mutation: Enhanced activation, basal [Ca2+]i and menthol response. *Neurol. Genet.* **7**, e550 (2021).
12. R. Gualdani *et al.*, ATRPM7 mutation linked to familial trigeminal neuralgia: Omega current and hyperexcitability of trigeminal ganglion neurons. *Proc. Natl. Acad. Sci. U.S.A.* **119**, e2119630119 (2022).
13. G. Di Stefano *et al.*, Familial trigeminal neuralgia–A systematic clinical study with a genomic screen of the neuronal electrogenisome. *Cephalalgia* **40**, 767–777 (2020).
14. J. Katz, One man's risk factor is another man's outcome: Difference in risk factor profiles for chronic postsurgical pain maintenance vs transition. *Pain* **153**, 505–506 (2012).
15. J. Katz, Z. Seltzer, Transition from acute to chronic postsurgical pain: Risk factors and protective factors. *Expert Rev. Neurother.* **9**, 723–744 (2009).
16. M. Moshirfar *et al.*, Neuropathic corneal pain following LASIK surgery: A retrospective case series. *Ophthalmol. Ther.* **10**, 677–689 (2021).
17. J. H. Yuan *et al.*, Genomic analysis of 21 patients with corneal neuralgia after refractive surgery. *Pain Rep.* **5**, e826 (2020).
18. D. E. Clapham, TRP channels as cellular sensors. *Nature* **426**, 517–524 (2003).
19. M. J. Caterina *et al.*, The capsaicin receptor: A heat-activated ion channel in the pain pathway. *Nature* **389**, 816–824 (1997).
20. D. Julius, TRP channels and pain. *Annu. Rev. Cell Dev. Biol.* **29**, 355–384 (2013).
21. S. E. Jordt, D. Julius, Molecular basis for species-specific sensitivity to "hot" chili peppers. *Cell* **108**, 421–430 (2002).
22. F. Yang *et al.*, Structural mechanism underlying capsaicin binding and activation of the TRPV1 ion channel. *Nat. Chem. Biol.* **11**, 518–524 (2015).
23. N. R. Gavva *et al.*, Molecular determinants of vanilloid sensitivity in TRPV1. *J. Biol. Chem.* **279**, 20283–20295 (2004).
24. M. Liao, E. Cao, D. Julius, Y. Cheng, Structure of the TRPV1 ion channel determined by electron cryo-microscopy. *Nature* **504**, 107–112 (2013).
25. E. Cao, M. Liao, Y. Cheng, D. Julius, TRPV1 structures in distinct conformations reveal activation mechanisms. *Nature* **504**, 113–118 (2013).
26. M. Tominaga *et al.*, The cloned capsaicin receptor integrates multiple pain-producing stimuli. *Neuron* **21**, 531–543 (1998).
27. R. Planells-Cases, N. Garcìa-Sanz, C. Morenilla-Palao, A. Ferrer-Montiel, Functional aspects and mechanisms of TRPV1 involvement in neurogenic inflammation that leads to thermal hyperalgesia. *Pflugers Arch.* **451**, 151–159 (2005).
28. G. Petho, P. W. Reeh, Sensory and signaling mechanisms of bradykinin, eicosanoids, platelet-activating factor, and nitric oxide in peripheral nociceptors. *Physiol. Rev.* **92**, 1699–1775 (2012).
29. D. H. Kwon *et al.*, Heat-dependent opening of TRPV1 in the presence of capsaicin. *Nat. Struct. Mol. Biol.* **28**, 554–563 (2021).
30. C. Belmonte, M. C. Acosta, J. Merayo-Lloves, J. Gallar, What causes eye pain? *Curr. Ophthalmol. Rep.* **3**, 111–121 (2015).
31. E. Aneiros *et al.*, The biophysical and molecular basis of TRPV1 proton gating. *EMBO J.* **30**, 994–1002 (2011).
32. T. Voets *et al.*, The principle of temperature-dependent gating in cold- and heat-sensitive TRP channels. *Nature* **430**, 748–754 (2004).
33. S. D. Dib-Hajj *et al.*, Transfection of rat or mouse neurons by biolistics or electroporation. *Nat. Protoc.* **4**, 1118–1126 (2009).
34. P. A. Koplas, R. L. Rosenberg, G. S. Oxford, The role of calcium in the desensitization of capsaicin responses in rat dorsal root ganglion neurons. *J. Neurosci.* **17**, 3525–3537 (1997).
35. G. Bhave *et al.*, cAMP-dependent protein kinase regulates desensitization of the capsaicin receptor (VR1) by direct phosphorylation. *Neuron* **35**, 721–731 (2002).
36. L. Sanz-Salvador, A. Andrés-Borderia, A. Ferrer-Montiel, R. Planells-Cases, Agonist- and Ca2+-dependent desensitization of TRPV1 channel targets the receptor to lysosomes for degradation. *J. Biol. Chem.* **287**, 19462–19471 (2012).
37. R. Kumar, M. Geron, A. Hazan, A. Priel, Endogenous and exogenous vanilloids evoke disparate TRPV1 activation to produce distinct neuronal responses. *Front. Pharmacol.* **11**, 903 (2020).
38. C. Belmonte, A. Aracil, M. C. Acosta, C. Luna, J. Gallar, Nerves and sensations from the eye surface. *Ocul. Surf.* **2**, 248–253 (2004).
39. K. Mizumura, T. Sugiura, K. Katanosaka, R. K. Banik, Y. Kozaki, Excitation and sensitization of nociceptors by bradykinin: What do we know? *Exp. Brain Res.* **196**, 53–65 (2009).
40. T. Sugiura, M. Tominaga, H. Katsuya, K. Mizumura, Bradykinin lowers the threshold temperature for heat activation of vanilloid receptor 1. *J. Neurophysiol.* **88**, 544–548 (2002).
41. X. Zhang, L. Li, P. A. McNaughton, Proinflammatory mediators modulate the heat-activated ion channel TRPV1 via the scaffolding protein AKAP79/150. *Neuron* **59**, 450–461 (2008).
42. S. Wang, J. Joseph, J. Y. Ro, M. K. Chung, Modality-specific mechanisms of protein kinase C-induced hypersensitivity of TRPV1: S800 is a polymodal sensitization site. *Pain* **156**, 931–941 (2015).
43. J. A. Matta, R. L. Miyares, G. P. Ahern, TRPV1 is a novel target for omega-3 polyunsaturated fatty acids. *J. Physiol.* **578**, 397–411 (2007).
44. P. M. Zygmunt *et al.*, Vanilloid receptors on sensory nerves mediate the vasodilator action of anandamide. *Nature* **400**, 452–457 (1999).
45. M. Patwardhan, P. E. Scotland, A. N. Akopian, K. M. Hargreaves, Activation of TRPV1 in the spinal cord by oxidized linoleic acid metabolites contributes to inflammatory hyperalgesia. *Proc. Natl. Acad. Sci. U.S.A.* **106**, 18820–18824 (2009).
46. M. Patwardhan *et al.*, Heat generates oxidized linoleic acid metabolites that activate TRPV1 and produce pain in rodents. *J. Clin. Invest.* **120**, 1617–1626 (2010).
47. J. Shin *et al.*, Bradykinin-12-lipoxygenase-VR1 signaling pathway for inflammatory hyperalgesia. *Proc. Natl. Acad. Sci. U.S.A.* **99**, 10150–10155 (2002).
48. S. W. Hwang *et al.*, Direct activation of capsaicin receptors by products of lipoxygenases: Endogenous capsaicin-like substances. *Proc. Natl. Acad. Sci. U.S.A.* **97**, 6155–6160 (2000).
49. K. Starowicz, S. Nigam, V. Di Marzo, Biochemistry and pharmacology of endovanilloids. *Pharmacol. Ther.* **114**, 13–33 (2007).
50. R. Kumar *et al.*, Activation of transient receptor potential vanilloid 1 by lipoxygenase metabolites depends on PKC phosphorylation. *FASEB J.* **31**, 1238–1247 (2017).
51. H. E. Bazan, D. L. Birkle, R. W. Beuerman, N. G. Bazan, Inflammation-induced stimulation of the synthesis of prostaglandins and lipoxygenase-reaction products in rabbit cornea. *Curr. Eye Res.* **4**, 175–179 (1985).
52. H. E. Bazan, Corneal injury alters eicosanoid formation in the rabbit anterior segment in vivo. *Invest. Ophthalmol. Vis. Sci.* **28**, 314–319 (1987).
53. H. E. Bazan, The synthesis and effects of eicosanoids in avascular ocular tissues. *Prog. Clin. Biol. Res.* **312**, 73–84 (1989).
54. N. G. Bazan, Metabolism of arachidonic acid in the retina and retinal pigment epithelium: Biological effects of oxygenated metabolites of arachidonic acid. *Prog. Clin. Biol. Res.* **312**, 15–37 (1989).
55. J. S. Hurst, M. Balazy, H. E. Bazan, N. G. Bazan, The epithelium, endothelium, and stroma of the rabbit cornea generate (12S)-hydroxyeicosatetraenoic acid as the main lipoxygenase metabolite in response to injury. *J. Biol. Chem.* **266**, 6726–6730 (1991).
56. H. E. Bazan, Y. Tao, M. A. DeCoster, N. G. Bazan, Platelet-activating factor induces cyclooxygenase-2 gene expression in corneal epithelium. Requirement of calcium in the signal transduction pathway. *Invest. Ophthalmol. Vis. Sci.* **38**, 2492–2501 (1997).
57. P. A. Mieyal, M. W. Dunn, M. L. Schwartzman, Detection of endogenous 12-hydroxyeicosatrienoic acid in human tear film. *Invest. Ophthalmol. Vis. Sci.* **42**, 328–332 (2001).
58. B. Wang *et al.*, Metabolism pathways of arachidonic acids: Mechanisms and potential therapeutic targets. *Signal Transduct. Target. Ther.* **6**, 94 (2021).
59. P. Rosenthal, D. Borsook, Ocular neuropathic pain. *Br. J. Ophthalmol.* **100**, 128–134 (2016).
60. D. Fakih *et al.*, Transient receptor potential channels: Important players in ocular pain and dry eye disease. *Pharmaceutics* **14**, 1859 (2022).
61. G. Callejo *et al.*, Acid-sensing ion channels detect moderate acidifications to induce ocular pain. *Pain* **156**, 483–495 (2015).
62. J. A. Belmonte, F. V. Brock, Converting cold into pain. *Exp. Brain Res.* **196**, 13–30 (2009).
63. R. Bron, R. J. Wood, J. A. Brock, J. J. Ivanusic, Piezo2 expression in corneal afferent neurons. *J. Comp. Neurol.* **522**, 2967–2979 (2014).
64. C. Belmonte, M. C. Acosta, J. Gallar, Neural basis of sensation in intact and injured corneas. *Exp. Eye Res.* **78**, 513–525 (2004).
65. K. H. Steen, A. E. Steen, P. W. Reeh, A dominant role of acid pH in inflammatory excitation and sensitization of nociceptors in rat skin, in vitro. *J. Neurosci.* **15**, 3982–3989 (1995).
66. Y. C. Woo, S. S. Park, A. R. Subieta, T. J. Brennan, Changes in tissue pH and temperature after incision indicate acidosis may contribute to postoperative pain. *Anesthesiology* **101**, 468–475 (2004).
67. K. H. Steen, P. W. Reeh, Sustained graded pain and hyperalgesia from harmless experimental tissue acidosis in human skin. *Neurosci. Lett.* **154**, 113–116 (1993).
68. M. C. Acosta, C. Belmonte, J. Gallar, Sensory experiences in humans and single-unit activity in cats evoked by polymodal stimulation of the cornea. *J. Physiol.* **534**, 511–525 (2001).
69. K. H. Steen, U. Issberner, P. W. Reeh, Pain due to experimental acidosis in human skin: Evidence for non-adapting nociceptor excitation. *Neurosci. Lett.* **199**, 29–32 (1995).
70. E. Deval *et al.*, Acid-sensing ion channels in postoperative pain. *J. Neurosci.* **31**, 6059–6066 (2011).
71. E. M. Pogatzki-Zahn, P. K. Zahn, T. J. Brennan, Postoperative pain–Clinical implications of basic research. *Best Pract. Res. Clin. Anaesthesiol.* **21**, 3–13 (2007).
72. N. Comes, X. Gasull, G. Callejo, Proton sensing on the ocular surface: Implications in eye pain. *Front. Pharmacol.* **12**, 773871 (2021).
73. P. Cesare, P. McNaughton, A novel heat-activated current in nociceptive neurons and its sensitization by bradykinin. *Proc. Natl. Acad. Sci. U.S.A.* **93**, 15435–15439 (1996).
74. L. S. Premkumar, G. P. Ahern, Induction of vanilloid receptor channel activity by protein kinase C. *Nature* **408**, 985–990 (2000).
75. H. Wen *et al.*, 20-Hydroxyeicosatetraenoic acid (20-HETE) is a novel activator of transient receptor potential vanilloid 1 (TRPV1) channel. *J. Biol. Chem.* **287**, 13868–13876 (2012).
76. G. Bhave *et al.*, Protein kinase C phosphorylation sensitizes but does not activate the capsaicin receptor transient receptor potential vanilloid 1 (TRPV1). *Proc. Natl. Acad. Sci. U.S.A.* **100**, 12480–12485 (2003).
77. M. Numazaki, T. Tominaga, H. Toyooka, M. Tominaga, Direct phosphorylation of capsaicin receptor VR1 by protein kinase C epsilon and identification of two target serine residues. *J. Biol. Chem.* **277**, 13375–13378 (2002).
78. L. E. Hains *et al.*, Pain intensity and duration can be enhanced by prior challenge: Initial evidence suggestive of a role of microglial priming. *J. Pain* **11**, 1004–1014 (2010).
79. A. E. Levitt *et al.*, Chronic dry eye symptoms after LASIK: Parallels and lessons to be learned from other persistent post-operative pain disorders. *Mol. Pain* **11**, 21 (2015).
80. D. S. Jacobs *et al.*, American academy of ophthalmology preferred practice pattern refractive management/intervention panel. Refractive surgery preferred practice pattern®. *Ophthalmology* **130**, P61–P135 (2023).
81. M. R. Ghovanloo *et al.*, Nav1.7 P610T mutation in two siblings with persistent ocular pain after corneal axon transection: Impaired slow inactivation and hyperexcitable trigeminal neurons. *J. Neurophysiol.* **129**, 609–618 (2023).
82. C. Theophanous, D. S. Jacobs, P. Hamrah, Corneal neuralgia after LASIK. *Optom. Vis. Sci.* **92**, 233–240 (2015).
83. J. F. Atkins *et al.*, A case for "StopGo": Reprogramming translation to augment codon meaning of GGN by promoting unconventional termination (Stop) after addition of glycine and then allowing continued translation (Go). *RNA* **13**, 803–810 (2007).
84. A. Luke *et al.*, Occurrence, function and evolutionary origins of "2A-like" sequences in virus genomes. *J. Gen. Virol.* **89**, 1036–1042 (2008).